Arctic freshwater export in the 20th and 21st centuries

Torben Koenigk,[1] Uwe Mikolajewicz,[1] Helmuth Haak,[1] and Johann Jungclaus[1]

Received 25 July 2006; revised 29 January 2007; accepted 21 March 2007; published 1 November 2007.

[1] Climate simulations suggest that the emissions of carbon dioxide and other greenhouse gases will lead to strong climate changes in the 21st century. Here the resulting effects of the freshwater balance of the Arctic Ocean in the 21st century are analyzed using coupled Intergovernmental Panel on Climate Change simulations with the Max Planck Institute for Meteorology climate model. For the Arctic region, particularly strong warming and an almost complete removal of sea ice during summer time are predicted. Arctic river runoff and net atmospheric freshwater input (P-E) are strongly enhanced. Most of this additional freshwater input is stored in the Arctic Ocean. While the total freshwater export out of the Arctic remains almost constant, significant changes occur in its distribution. The dominance of sea ice for the Fram Strait export disappears, while the liquid freshwater export is enhanced. The mean export shows therefore almost no changes, but its interannual variability is slightly reduced. In contrast, both the export through the Canadian Archipelago and its variability are increased in the 21st century. Therefore the importance of the Canadian Archipelago for the total Arctic export grows. Enhanced freshwater input into the Labrador Sea leads to a strong decrease in deep convection. Greenland Sea convection is reduced as well but mainly because of strong warming of the upper ocean layers. The meridional overturning circulation responds with a decline of about 6 sverdrups.

Citation: Koenigk, T., U. Mikolajewicz, H. Haak, and J. Jungclaus (2007), Arctic freshwater export in the 20th and 21st centuries, *J. Geophys. Res.*, *112*, G04S41, doi:10.1029/2006JG000274.

1. Introduction

[2] The Arctic plays an important role in the global climate system. As an interface between atmosphere and ocean, the rather thin layer of sea ice controls most of the fluxes of heat, momentum and matter in ice-covered regions. Small changes in sea ice cover may have a strong impact on the large-scale atmospheric circulation [*Magnusdottir et al.*, 2004; *Alexander et al.*, 2004].

[3] The export of freshwater from the Arctic is very important for the coupling of the Arctic Ocean to the rest of the world. This export influences and alters the deep water formation in the North Atlantic Ocean, in particular in the Labrador Sea. The largest source of export is the Fram Strait sea ice export. It amounts to about 2400–3200 km^3/a (75,000–100,000 m^3/s) [*Vinje et al.*, 1998; *Vinje*, 2001; *Aargaard and Carmack*, 1989; *Schmith and Hansen*, 2003]. The interannual variability of the ice export is large and mainly dominated by the sea level pressure gradient across Fram Strait. According to *Vinje* [2001] and *Hilmer et al.* [1998], this pressure gradient explains more than 80% of the total variability of the ice export. Several investigations indicated that large ice export events strongly reduce the convection in the Labrador Sea 1 or 2 a later. *Dickson et al.* [1988] and *Belkin et al.* [1998] suggested that at least the so-called "Great Salinity Anomaly" (GSA) in the early 70s was caused by previous large Fram Strait sea ice exports. *Häkkinen* [1999] prescribed large freshwater anomalies in the East Greenland Current and showed that they provoke GSAs in the Labrador Sea. *Haak et al.* [2003] performed simulations with an ocean model forced by NCEP reanalyses and found that also the GSAs of the 80s and 90s are caused by large sea ice exports. *Koenigk et al.* [2006] showed a significant atmospheric response to large sea ice export events through Fram Strait.

[4] The most important source of freshwater for the Arctic Ocean is river runoff. *Peterson et al.* [2002] analyzed river-monitoring data of the largest 6 Eurasian rivers from 1936 to 1999 and found an increase of 7% in the discharge. *Berezovskaya et al.* [2005] showed an increase in runoff of the Lena River by 10% since 1936 with particularly high runoff since 1988. The authors attributed this to strong precipitation to an anomalously positive Arctic Oscillation (AO). In contrast to the enhanced river runoff in Eurasia, the river discharge in northern Canada decreased by 10% since 1964 [*Déry and Wood*, 2005]. *Dyurgerov and Carter* [2004] analyzed mass balance data from Arctic mountains and subpolar glaciers. They came to the conclusion that melting of glaciers was the main source of increased freshwater inflow into the Arctic Ocean since 1961. In agreement with these observations, *Wu et al.* [2005] simulated an increased river runoff in the second part of the 20th century with the HadCM3 model.

[1] Max-Planck-Institut für Meteorologie, Hamburg, Germany.

0148-0227/07/2006JG000274

[5] As found both in satellite observations [*Kwok*, 2000] and model studies [*Hilmer and Lemke*, 2000], sea ice cover has strongly reduced over the last 30 a as well. *Serreze et al.* [2000] suggested that about half of the observed changes in the Arctic can be attributed to changes in the atmospheric circulation. This would explain the warmer and wetter climate in Siberia and the colder and drier climate in northern Canada at the same time. The second half of the changes may be attributed to anthropogenic forcing. Data records are still quite short and model simulations suggest a large decadal to multidecadal variability in the Arctic [e.g., *Goosse et al.*, 2002; *Jungclaus et al.*, 2005]. Therefore the interpretation of the change as a signal for enhanced greenhouse warming is still under debate. However, model simulations predict a future climate change in the Arctic that is amplified because of ice-albedo feedback [*Holland and Bitz*, 2003].

[6] In this study, an ensemble of Intergovernmental Panel on Climate Change (IPCC) scenario runs performed with the global coupled atmosphere-ocean model ECHAM5/MPI-OM is analyzed. The freshwater export from the Arctic in the 20th and 21st century is investigated. The reasons for the changes and their possible impacts are presented.

2. Model Description

[7] The model used in this study is the Max Planck Institute for Meteorology global atmosphere–ocean–sea ice model ECHAM5/MPI-OM. It consists of the latest (fifth) cycle of the European Centre for Medium-Range Weather Forecasts Hamburg (ECHAM) and Max Planck Institute Ocean Model (MPI-OM). The atmosphere model ECHAM5 [*Roeckner et al.*, 2003] is run at T63 resolution, which corresponds to a horizontal resolution of about 1.875° × 1.875°. It has 31 vertical levels up to 10 hPa. The ocean model MPI-OM [*Marsland et al.*, 2003; *Jungclaus et al.*, 2006] includes a Hibler-type dynamic-thermodynamic sea ice model. The ocean grid is based on an Arakawa C grid and allows for an arbitrary placement of the grid poles. In this setup, the model's North Pole is shifted to Greenland and the South Pole is placed in the center of Antarctica. This approach avoids the numerical singularity at the North Pole. It has the additional advantage of a relatively high resolution in the deep water formation regions near Greenland and in the Weddell Sea. The grid spacing varies between about 15 km around Greenland and 184 km in the tropical Pacific. The model has 40 vertical layers.

[8] The atmosphere model and the sea ice–ocean model are coupled by the OASIS coupler [*Valcke et al.*, 2003]. The coupler transfers fluxes of momentum, heat, and freshwater from the atmosphere to the ocean and performs the interpolation onto the ocean grid. It also transmits sea surface temperature, sea ice thickness and concentration, snow thickness and surface velocity from the ocean to the atmosphere. The climate model includes a river runoff scheme [*Hagemann and Duemenil*, 1998; *Hagemann and Duemenil-Gates*, 2003]. The river runoff is transferred to the ocean together with the precipitation. Glacier calving is included such, that any snow falling on Greenland and Antarctica is instantaneously transferred into the nearest ocean grid point. Hence the mass balance of glacier ice sheets is not accounted for. In the coupled model, no flux adjustment is used.

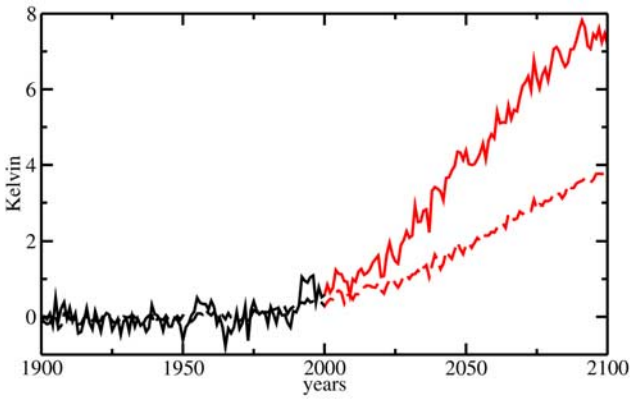

Figure 1. Annual mean 2 m air temperature anomalies in Kelvin. Ensemble means of the 20th century and A1B scenario runs are shown. The dashed line shows the global average, and the solid line shows the average of the area north of 60°N.

[9] In this study, simulations of the climate during the 20th and 21st century are analyzed. For the 20th century runs, observed concentrations of climate relevant gases and aerosols are used. For the 21st century, the IPCC scenario A1B is prescribed. A detailed description of the IPCC scenarios is given in the IPCC Special Report on Emission Scenarios (SRES: http://www.ipcc.ch/). Solar variability is not considered in the simulations.

[10] An ensemble of three members is used both for the 20th and 21st century runs. The three realizations of the 20th century have been started with initial conditions from three different years of a preindustrial control integration. The 21st century simulations were started from the end of the three 20th century runs. It should be noted that the cooling effect of aerosols exceeds the warming due to increased CO_2 in the Arctic in large parts of the 20th century. For this period, the 20th century runs present a slightly colder Arctic climate than the control runs. This leads to somewhat enhanced ice exports and reduced liquid freshwater exports in the 20th century simulations. In the following, ensemble means are presented.

3. Results

3.1. Changes in the Arctic Climate

[11] This subsection analyses the changes of relevant parameters of the Arctic freshwater system. Figure 1 shows ensemble mean air temperature anomalies of the area-weighted global mean and the mean of the area north of 60°N in the 20th and 21st centuries. The warming in the Arctic reaches more than 7 K by the year 2100, which is almost twice the global mean warming. The main reason is the ice-albedo feedback: A warming leads to an increased melting of sea ice in the Arctic. This reduces the albedo and more solar radiation will be absorbed. Consequently, the warming is enhanced.

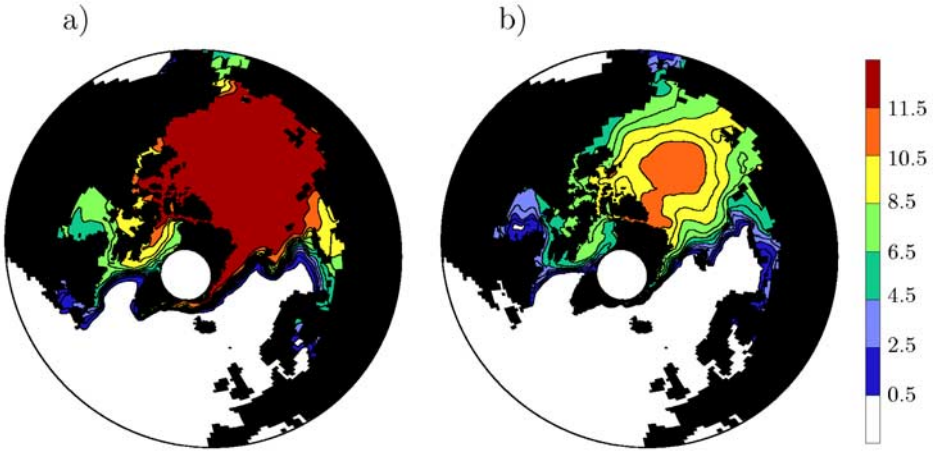

Figure 2. Annual number of months with a sea ice concentration exceeding 15%. (a) Mean of 1900–2000. (b) Mean of 2080–2100. Shown are ensemble means.

[12] The decrease of Arctic sea ice coverage can be seen in Figure 2. In the 20th century, almost the entire Arctic Ocean is ice-covered year round. Only the Barents Sea and parts of the Kara Sea are ice free during summertime. The model reproduces satellite observations [*Johannessen et al.*, 2002] in most areas reasonably well. However, at the coasts of the Laptev and East Siberian seas, sea ice thickness and summer sea ice cover are slightly overestimated. During the 21st century, sea ice is strongly reduced. At the end of the century, the Arctic is completely ice free during a short period in summer. There is no region with an ice cover duration exceeding 11.5 months. During wintertime, the Arctic is still ice covered and the reduction of maximal sea ice extent is rather moderate. However, the ice volume is strongly reduced in winter as well. The difference between winter and summer ice volume in the Arctic remains constant as do winter ice production rates in the entire 21st century.

[13] Exchange processes with the atmosphere are of great importance for the freshwater balance of the ocean. Figure 3a shows the averaged atmospheric net freshwater input into the ocean in the 20th century, which is given by the difference between evaporation (E) and precipitation (P). On the right, the difference of E-P averaged from 2080 to 2100 and from 1900–000 (Figure 3b) is presented. Most parts of the Arctic are dominated by an excess of P over E in the 20th century. *Groves and Francis* [2002] analyzed a 19-a data set and found similar results. They showed that the annual E-P pattern is dominated by E-P in summer. In our model, the annual mean excess of precipitation varies between 10 and 30 mm/month over the Arctic Ocean and more than 80 mm/month over the North Pacific, the western North Atlantic and in some coastal regions. Positive E-P values occur over parts of the Norwegian and southwestern Barents Sea. Here, a combination of relatively warm surface water and strong winds leads to strong evaporation, especially in winter when cold Arctic air masses are advected over the open ocean. The changes until the period 2080–2100 are characterized by a growing difference of P-E in large parts of the Arctic. This increase reaches 2–10 mm/month in most areas. Again, over

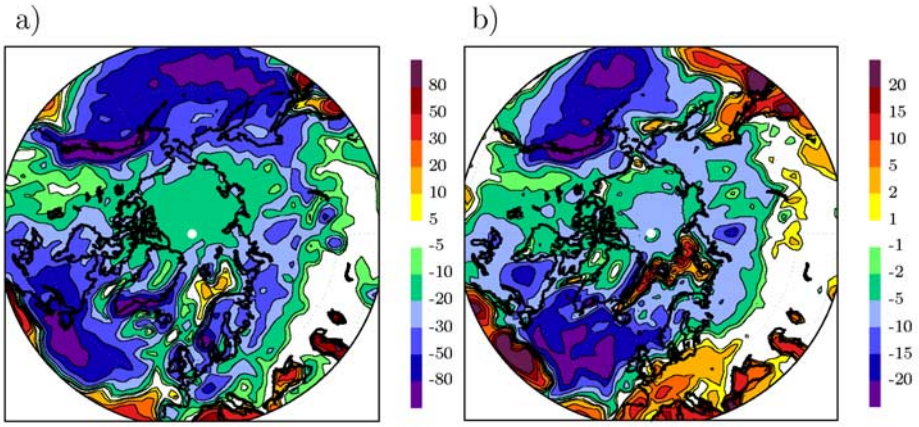

Figure 3. (a) Annual mean E-P during 1900–2000 in mm/month. (b) E-P difference between the means of 2080–2100 and 1900–2000. Shown are ensemble means.

the North Atlantic and North Pacific larger values occur. In an area along the displaced ice edge from Iceland over Spitsbergen to the Kara Sea, evaporation is strongly enhanced because of the reduction of sea ice during winter. The net atmospheric freshwater input into the Arctic Ocean (including Barents Sea) grows from about 70,000 m^3/s in the 20th century (mean 1900–2000) to slightly more than 80,000 m^3/s at the end of the 21st century (Figure 4a). As only rather few observational records exist for the Arctic, it is difficult to provide safe observational estimates. *Walsh et al.* [1994] and *Serreze et al.* [1995] have utilized the network of northern high-latitude rawinsonde stations to examine P-E averaged over the Arctic Basin north of 70°N. They found mean values for a 20-a time period of about 160–170 mm/a, which is equivalent to a net atmospheric freshwater flux of about 80,000 m^3/s for the area north of 70°N. Note that we only use the Arctic Ocean (including Barents Sea) as Arctic, which slightly differs from the area north of 70°N used by *Walsh et al.* [1994] and *Serreze et al.* [1995].

[14] The river runoff to the Arctic Ocean reaches on average about 130,000 m^3/s in our 20th century simulations. This agrees with results of *Lammers et al.* [2001] and *Peterson et al.* [2002]. They analyzed river discharge data of the 20th century and found a runoff to the Arctic Ocean of 130,000 m^3/s and 152,000 m^3/s, respectively. Several observational studies [*McClelland et al.*, 2004, 2006; *Berezovskaya et al.*, 2004] showed a positive trend of both P and river runoff in the second half of the 20th century. However, *Berezovskaya et al.* [2004] analyzed three different precipitation data sets and found that the observed P trend seems to be too weak to explain the strong increase in river runoff. *McClelland et al.* [2004] analyzed the impact of dams, permafrost thaw and fires on the Siberian river runoff but could not explain the significant increase in river runoff. He concluded that increasing northward transport of moisture as a result of global warming remains the most viable explanation for the observed increase in Eurasian Arctic river discharge. Contrary to P in Siberia, it seems P was not enhanced in northern Canada since 1950: *Déry and Wood* [2005] found a decrease both in P and river runoff. Using station data, *Przybylak* [2002] showed a reduction in P in the southeastern Canadian Arctic otherwise P was increased. Model results by *Wu et al.* [2005] with the HadCM3 climate model showed a rise of the total Arctic river runoff by about 10,000 m^3/s since 1960. Main reason for this was increasing precipitation over Siberia whereas changes in the discharge of the North American rivers contributed only little to the positive trend. Our simulations show an enhanced Eurasian river runoff by 5000 m^3/s between 1960 and 2000. This is somewhat less than in the simulations by *Wu et al.* [2005]. The increase in our simulations fits well to increased P in the catchment areas of the Eurasian rivers in our model. Hence our simulations do not show the gap between precipitation and river runoff trend as shown by *Berezovskaya et al.* [2004]. It has to be noted that our river runoff scheme does not include changes due to permafrost thaw, vegetation changes and human activities. In contrast to Siberia, river discharge of the North American rivers does not change throughout the 20th century in our simulations.

[15] During the 21st century, our simulation show a growing excess of P over E in the catchment areas of both the Siberian and Canadian rivers. The total river discharge grows to 170,000 m^3/s by the year 2100. Other model simulations show similar results. Simulations by *Wu et al.* [2005] until year 2050 following the B2 and A2 scenarios predict a further rise of river runoff. *Arnell* [2005] used a hydrological model forced with climate change scenarios and found an increase of 24 to 31% until 2080. Simulations with a coupled ocean-atmosphere-land model by *Manabe et al.* [2004] showed an increase of about 20% until year 2100. In our simulations, the total runoff (river runoff plus P-E, Figure 4a), increases by about 50,000 m^3/s until the year 2100.

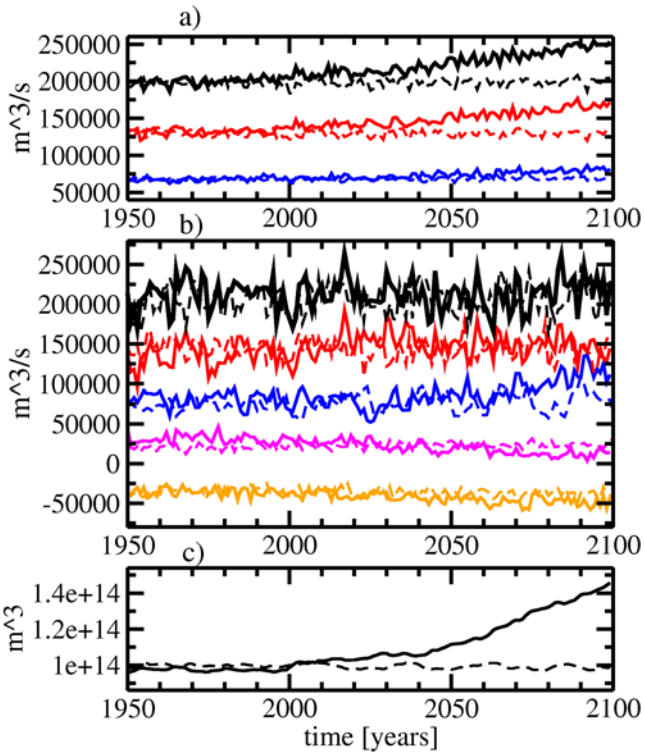

Figure 4. (a) Annual mean Arctic river runoff (red), P-E over the Arctic Ocean (blue), and total Arctic runoff (river runoff plus P-E, black) in m^3/s. (b) Annual mean freshwater export through Fram Strait (red), Canadian Archipelago (blue), Barents Shelf (magenta), Bering Strait (orange), and total export out of the Arctic (black) in m^3/s. (c) Annual mean freshwater content of the Arctic Ocean in m^3. The dashed lines are the ensemble means of the control runs.

3.2. Changes in the Arctic Freshwater Exports

[16] The model results indicate that increased P-E and river runoff will lead to an enhanced freshwater flux into the Arctic Ocean during the 21st century. In the following, we investigate how this influences freshwater exports from the Arctic.

[17] Equation (1) is used to calculate the liquid freshwater export Q. Calculations of the ice export are done with a sea ice salinity of 5 psu. The common reference salinity of 34.8 is used for all calculations in this study. The results are tested against changes in the reference salinity. It turns out that the conclusions are independent from the reference

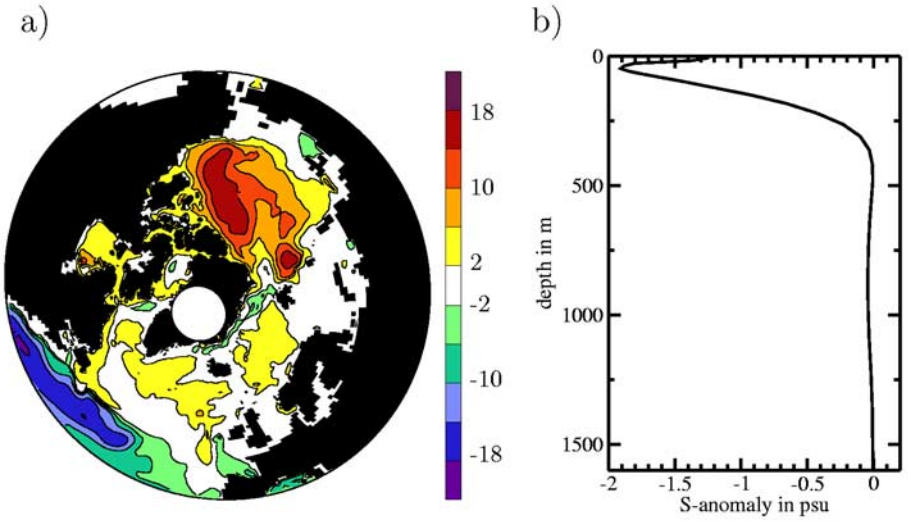

Figure 5. (a) Ensemble mean freshwater content differences between the periods 2080–2100 and 1950–2000 in m. (b) S differences averaged over the Arctic Ocean between 2080–2100 and 1950–2000.

salinity, while the amounts of the freshwater exports change:

$$Q = \int_{z=B}^{T} \int_{x=x0}^{x1} u\left(\frac{Sref - S}{Sref}\right) dxdz \qquad (1)$$

where B = bottom, T = surface or sea ice bottom line; x0, x1 = end points of section; u = velocity perpendicular to section; *S*, *Sref* = salinity and reference salinity.

[18] Figure 4b shows the total (liquid plus solid) freshwater export out of the Arctic for all passages averaged over the three ensemble runs. The dashed lines show the ensemble means of the control runs. The largest export takes place through Fram Strait. In the 20th century it is 136,000 m^3/s on average. This agrees well with observational estimates of *Aargaard and Carmack* [1989] and *Dickson et al.* [2007], who found values of 115,000 and 150,000 m^3/s, respectively. In our simulation, a small positive trend can be seen until 2030, with a decrease afterward. Hence the export at the end of the 21st century shows only a very weak increase compared to the average of the 20th century. In contrast, the export through the Canadian Archipelago is strongly enhanced in the second half of the 21st century. It increases from about 80,000 m^3/s to approximately 110,000 m^3/s. Only few observations of the export through the Canadian Archipelago exist. *Prinsenberg and Hamilton* [2005] measured the freshwater export through Lancaster Sound for 3 a and found a mean export of 45,000 m^3/s. They suggested that the export through Lancaster Sound makes up 35–50% of the freshwater fluxes through the entire Canadian Archipelago.

[19] Our simulations show a reduced net export over the Barents Shelf (borderline from southeast Svalbard (78°N, 24°E) to North Cape (71°N, 28°E)) and a positive trend of freshwater import through Bering Strait in the 21st century. The import through Bering Strait in the 20th century (36,000 m^3/s on average) seems to be somewhat too small compared to observational estimates by *Woodgate and Aagaard* [2005].

[20] The total freshwater export out of the Arctic basin consists of the sum of these four exports. Over the entire model period, changes in the Arctic export are quite small. The enhanced export through the Canadian Archipelago is almost totally compensated for by the decreasing export over the Barents Shelf and the growing import through Bering Strait. Since the freshwater export from the Arctic changes only slightly, the additional input by P-E and river runoff must be stored in the Arctic Ocean itself. Figure 4c shows that the freshwater content is indeed strongly increased in the 21st century. The mean of the three realizations gives an increase of about 45% of the total freshwater content until the year 2100. The three members vary from each other by up to 5% for decadal means. For example, the freshwater content in one of the members is about 5000 km^3 higher than the other two during 2040 and 2060 and again higher between 2075 and 2100.

[21] Figure 5 shows the vertical and horizontal distribution of the additional freshwater storage in the Arctic Ocean. The salinity change until the end of the 21st century, averaged over the Arctic Ocean for each vertical layer, is presented on the right side (Figure 4b). Most of the freshwater is stored between the surface and 250 m depths. The largest basin mean salinity anomaly of almost 2 psu occurs around 50 m depth. The spatial distribution of the freshwater content anomaly (Figure 5a) indicates a strong freshwater increase in the Central Arctic and the Beaufort Sea of up to 15 m. Along the Siberian coast and in the Barents Sea, anomalies remain small.

[22] As shown above, by far the largest freshwater exports take place through Fram Strait and the Canadian Archipelago. In the following, they are analyzed in detail. The exports are divided into their solid and liquid part (Figures 6a and 6b). In the 20th century, on average 83,000 m^3/s of the freshwater export through Fram Strait is solid. This is slightly more than in the control runs because of a colder Arctic climate. *Vinje* [2001] and *Aargaard and Carmack* [1989] found similar results for the 20th century. During the 21st century, the ice export is strongly reduced

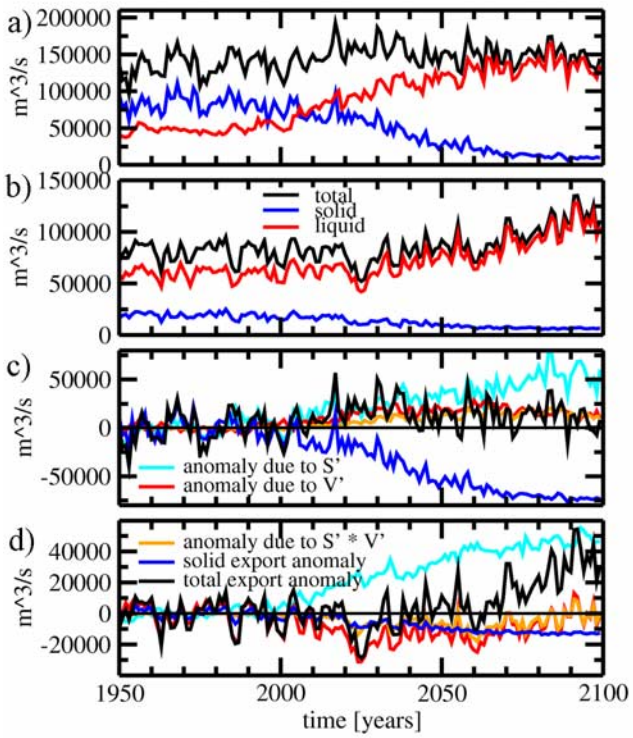

Figure 6. (a) Ensemble means of annual mean total (black), solid (blue), and liquid (red) freshwater exports through Fram Strait in m^3/s. (b) Same as Figure 6a but for the Canadian Archipelago. (c) Ensemble means of anomalous freshwater export through Fram Strait in m^3/s. The export anomalies are divided into anomalies related to salinity change and volume flux change and to change in the ice export. The anomaly of the total export is shown in black. The reference period for the anomalies is 1950–2000. (d) Same as Figure 6c but for the Canadian Archipelago.

and almost zero at the end of the century because of the melting of sea ice in the Arctic Ocean (compare Figure 2). The liquid part in the 20th century simulations is slightly smaller than that in the control run. It amounts to about two third of the ice export. This agrees well with results of *Holfort and Meincke* [2005] who measured the freshwater transport on the East Greenland Shelf at 74°N. The interannual variability of the liquid transport is small compared to the ice export. In the 21st century both the mean liquid export and variability are strongly enhanced.

[23] The interannual variability of the total export through Fram Strait is dominated by ice export in the 20th century. Their correlation exceeds 0.9. This changes during the 21st century, where the liquid part increasingly governs the variability of the total freshwater export.

[24] In the Canadian Archipelago, the solid export decreases and almost disappears to the end of the 21st century as well (Figure 6b). The liquid export is much larger than the solid and it increases from about 60,000 m^3/s to more than 100,000 m^3/s by 2100. In contrast to the export through Fram Strait, the variability of the total export through the Canadian Archipelago is governed by the liquid part in the 20th century. This dominance of the liquid part increases further during the 21st century.

[25] Although the three realizations of the exports through Fram Strait and Canadian Archipelago show a similar statistical behavior, they differ from each other quite substantially during certain time periods. The same ensemble member that shows the largest freshwater content during 2040–2060 has the smallest Fram Strait export in this period. It then reaches on average 120,000 m^3/s. The means of the other two realizations for this period are 147,000 m^3/s and 170,000 m^3/s, respectively. The run with the largest Fram Strait export during 2040–2060 shows by far the smallest export through the Canadian Archipelago. The mean of 2040–2060 is only 73,000 m^3/s, while the other realizations reach about 90,000 m^3/s. Hence the single ensemble members can vary from each other by 30% for periods of one to three decades.

[26] Figures 6c and 6d underline the importance of anomalies in salinity, volume flux and ice export for the total export through Fram Strait and the Canadian Archipelago. The liquid freshwater anomaly is divided into anomalies related to salinity anomalies ($S'\underline{V}$), volume flux anomalies ($V'\underline{S}$), and the product of salinity and volume flux anomalies ($S'V'$). Here, S is the difference between reference salinity (34.8 psu) and simulated salinity divided by the reference salinity ($S = (Sref - Ssim)/Sref$). The anomalies (S', V') are calculated in reference to the mean of the time period 1950–2000 ($\underline{S}$, $\underline{V}$). In Fram Strait (Figure 6c), the anomalies of the total export are dominated by ice export anomalies in the 20th century. Until 2030, both $S'\underline{V}$ and $V'\underline{S}$ are positive and lead to an enhanced total export. The ice export is reduced by about 20,000 m^3/s until 2030 but is still highly correlated with the total export. After 2030 the ice export is strongly reduced and reaches negative anomalies of more than −70,000 m^3/s. $S'\underline{V}$ continues its positive trend and its anomaly amounts to more than 50,000 m^3/s by the year 2100. After the strong decrease of sea ice, the salinity of the water, exported through Fram Strait, governs the variability of the total export. $V'\underline{S}$ stays positive but it is slightly decreased toward the end of the century. $S'V'$ accounts for an anomaly of about 15,000 m^3/s and because of a reduced salinity and thus larger S′, the interannual variability of $S'V'$ is enhanced. Altogether, the total export anomaly does not reach more than 5000 m^3/s at the end of the century.

[27] In the 20th century, anomalies of the total freshwater export through the Canadian Archipelago are mainly dominated by the variability of the volume flux ($V'\underline{S}$). The ice export is positively correlated to $V'\underline{S}$ and increases the anomalies, while $S'\underline{V}$ and particularly $S'V'$ are quite small. Hence the salinity of the exported water does not vary strongly and has only a small impact on the variations of the total export. Until 2025, $V'\underline{S}$ decreases by 20,000 m^3/s. Also sea ice export anomalies and $S'V'$ are negative while the salinity related anomalies show a positive trend. This positive trend continues until the end of the century and $S'\underline{V}$ reaches almost 50,000 m^3/s. This fits well to the accumulation of freshwater northeast of Greenland (Figure 5). $V'\underline{S}$ and $S'V'$ stay constant until 2060. Thereafter, they have a positive trend and reach 0 to the end of the century. They are highly positively correlated in the second half of the 21st century as the variability of $S'V'$ is also dominated by V'. The variability of the salinity does not change much. However, salinity is strongly reduced which is why the

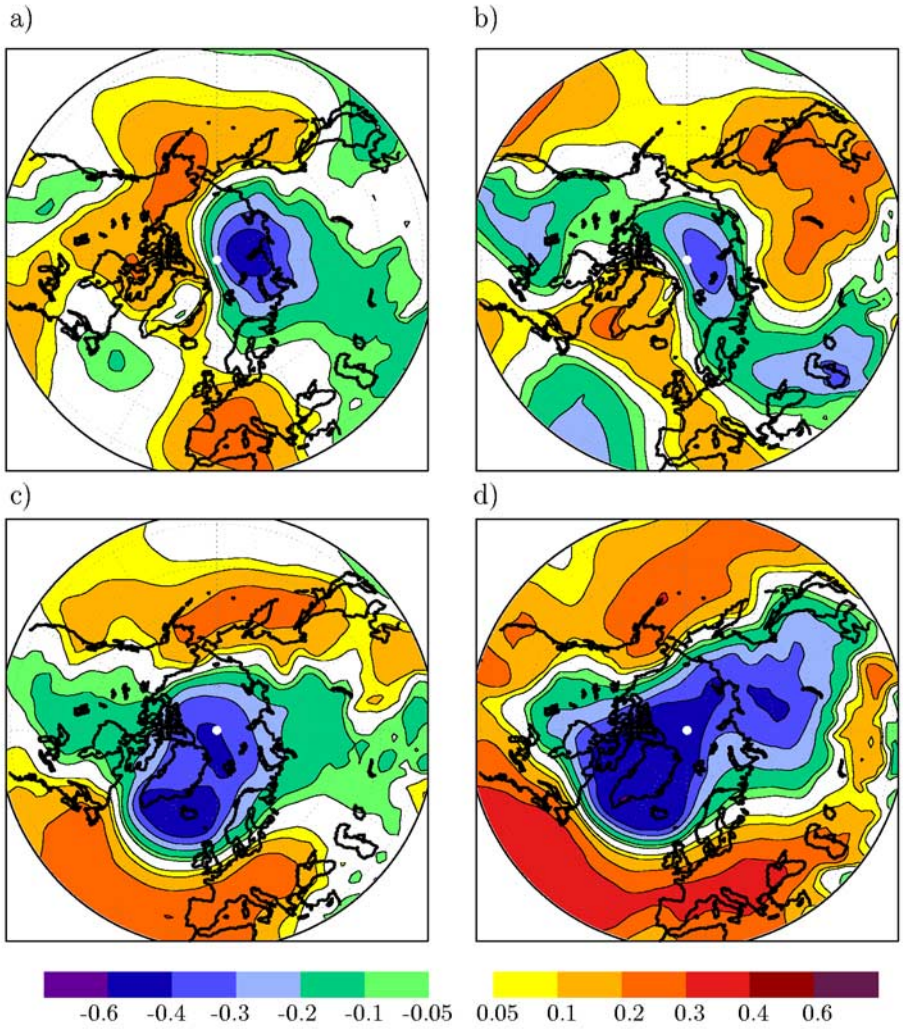

Figure 7. Correlation between annual mean total freshwater export through Fram Strait and SLP for (a) 1950–2000 and (b) 2080–2100. (c and d) Same as Figures 7a and 7b for the Canadian Archipelago.

amount of S' becomes larger. Consequently, the variations of $S'\,V'$ are enhanced. The total export is strongly increased from 2060 onward. However, although the positive trend in the export through the Canadian Archipelago is caused by the reduction of salinity ($S'\,\underline{V}$), the interannual variability is mainly dominated by variations of the volume flux ($V'\,\underline{S}$) for the entire period.

[28] Several investigations [*Vinje*, 2001; *Hilmer et al.*, 1998] have shown that the local wind forcing in the Fram Strait governs the interannual variability of the ice export. In the second part of the 20th century this local forcing was dominated by the NAO [*Hilmer and Jung*, 2000]. However, this relationship seems to be unstable [*Jung and Hilmer*, 2001]. *Cavalieri* [2002] and *Cavalieri and Häkkinen* [2001] suggested a stable connection between local wind in Fram Strait and the phase of wave number 1 of Arctic sea level pressure (SLP). Figure 7 shows the correlation between the total freshwater export through Fram Strait and SLP (top) and between the Canadian Archipelago and SLP (bottom) for the periods 1950–2000 and 2080–2100. Fram Strait freshwater export is highly negatively correlated with SLP over Kara and Laptev seas. Positive correlations occur over Alaska and northern Canada and also over southwestern Europe. A strong SLP gradient across the Arctic and Fram Strait leads to enhanced sea ice transports to Fram Strait and through it [*Koenigk et al.*, 2006]. The correlation between SLP gradient across Fram Strait and ice export reaches 0.7 in the 20th century; the total export and SLP gradient are correlated with 0.58. By the end of the 21st century, the correlation pattern between freshwater export and SLP has changed. Over the Kara Sea, correlations still reach −0.4 but the strong SLP gradient across the Arctic has weakened. Now, freshwater is mainly transported from the Beaufort Sea toward Fram Strait. This fits well to the accumulation of freshwater in Beaufort Sea (Figure 5a), which leads to a low salinity there. Therefore freshwater coming from the Beaufort Sea to Fram Strait strongly enhances the Fram Strait freshwater export. The correlation between SLP gradient over Fram Strait and freshwater export has weakened as well and amounts to 0.48. The reduction is mainly due to the loss of sea ice, which reacts especially sensitive to the wind. The high correlation between freshwater export and SLP gradient in the 20th century was due to the high correlation between sea ice export and wind forcing. The

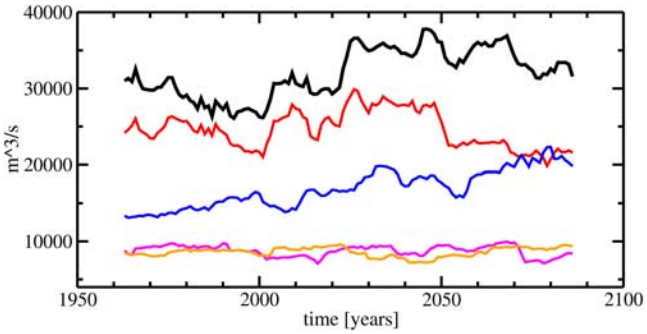

Figure 8. Standard deviation of running 25-a periods of the annual mean freshwater exports through Fram Strait (red), Canadian Archipelago (blue), Barents Shelf (magenta), and Bering Strait (orange) and the total export out of the Arctic (black) in m^3/s. Shown are ensemble means.

liquid freshwater export through Fram Strait showed only a very weak correlation to the SLP gradient. However, as the upper ocean layers at the end of the 21st century are more directly influenced by the wind because of the lack of sea ice, a significant correlation remains.

[29] The correlation analysis between the freshwater export through the Canadian Archipelago and SLP shows for the 20th and the 21st century a pronounced NAO pattern. During a positive NAO, the wind transports water into the Canadian Archipelago and out of the Labrador Sea, which increases the sea surface height gradient and leads to a stronger transport through the Archipelago. The correlation between NAO index and freshwater export through the Canadian Archipelago is 0.43 in the 20th century and increases slightly to 0.46 in the 21st century.

[30] Besides the amount of freshwater export, also the variability is of relevance for the climate system. To analyze the development of the interannual variability throughout the entire period, the standard deviation of annual exports of running 25-a periods was calculated. This was done individually for each of the three ensemble runs before calculating the mean of the three runs (Figure 8). The standard deviation of the Fram Strait freshwater export is by far largest (about 25,000 m^3/s) in the 20th century. It exhibits a positive trend between 2000 and 2030 and decreases thereafter to about 21,000 m^3/s at the end of the century. Although, the differences between the ensemble members are quite large (not shown), the reduction in the interannual variability in the second half of the 21st century seems to be robust. The variability of the export through the Canadian Archipelago shows a positive trend throughout the entire period. The ensemble mean standard deviation increases from slightly below 15,000 m^3/s to more than 20,000 m^3/s at the end of the 21st century and is then of the same size as the standard deviation of the Fram Strait export. The enhanced variability is mainly caused by an increased variability of $S' V'$ (Figure 6). The exports through Fram Strait and Canadian Archipelago are slightly negatively—but not significantly—correlated in the 20th century. During the 21st century, there is no correlation at all. The standard deviations of the exports through Bering Strait and over the Barents Shelf do not vary very strongly and do not show any significant trend.

[31] The variability of the entire Arctic freshwater export is dominated by the variability in Fram Strait export in the 20th century. The correlation between the exports through Fram Strait and out of the total Arctic is 0.83 for the period 1950–2000. During the 21st century the correlation is slightly reduced to 0.71 for the period 2050–2100. In contrast, the correlations between Canadian Archipelago and total Arctic exports are 0.36 and 0.56, respectively. As a consequence, the variability of the total Arctic export does not follow the negative trend of the variability in Fram Strait but remains constant in the second half of the 21st century.

3.3. Impact on the Atlantic Meridional Overturning Circulation

[32] In the following, we focus on possible impacts of the changing freshwater exports on climate. Several investigations showed that convection in the North Atlantic is very sensitive to changes in the freshwater balance. For example, *Häkkinen* [1999] simulated idealized freshwater pulses in the East Greenland Current, which led to reduced convection in the Labrador Sea. *Mauritzen and Häkkinen* [1997] used a fully coupled ocean-sea ice model to perform two runs with different ice exports through Fram Strait. The meridional overturning circulation responded with a reduction to an increased ice export.

[33] Here, we separately analyze the convection in the Labrador and the Greenland Sea. A convection index is formed by spatially integrating the mixed layer depth over the convection areas of the Greenland and Labrador Sea. For better comparison, the index is normalized. Figure 9a) shows the time series of the convection index for both areas. It is reduced by 50% in the Labrador Sea and by 35% in the Greenland Sea during the 21st century. The main reduction takes place between the years 2000 and 2060. Thereafter, the index is not changing much anymore. *Wood et al.* [1999] analyzed the spatial structure of the thermohaline circulation in response to atmospheric forcing in the HadCM3 climate model. In their model, CO_2 forcing leads to a collapse of

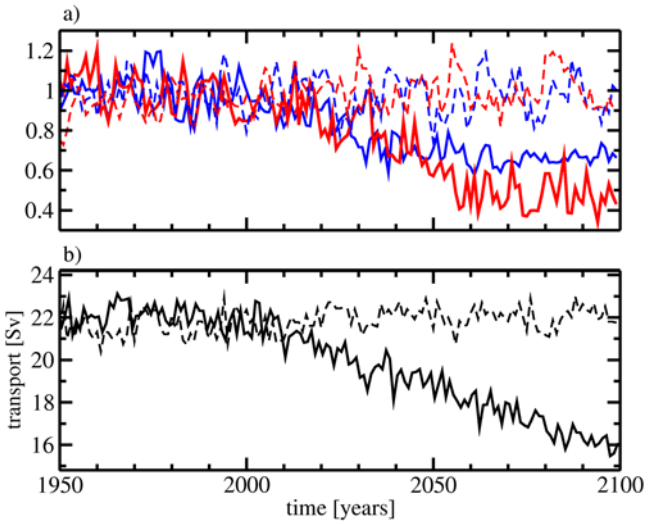

Figure 9. (a) Normalized integral of the mixed layer depth over the Labrador (red) and Greenland Sea (blue) convection areas. (b) Maximal Atlantic MOC in sverdrups. The dashed lines show ensemble means of the control runs.

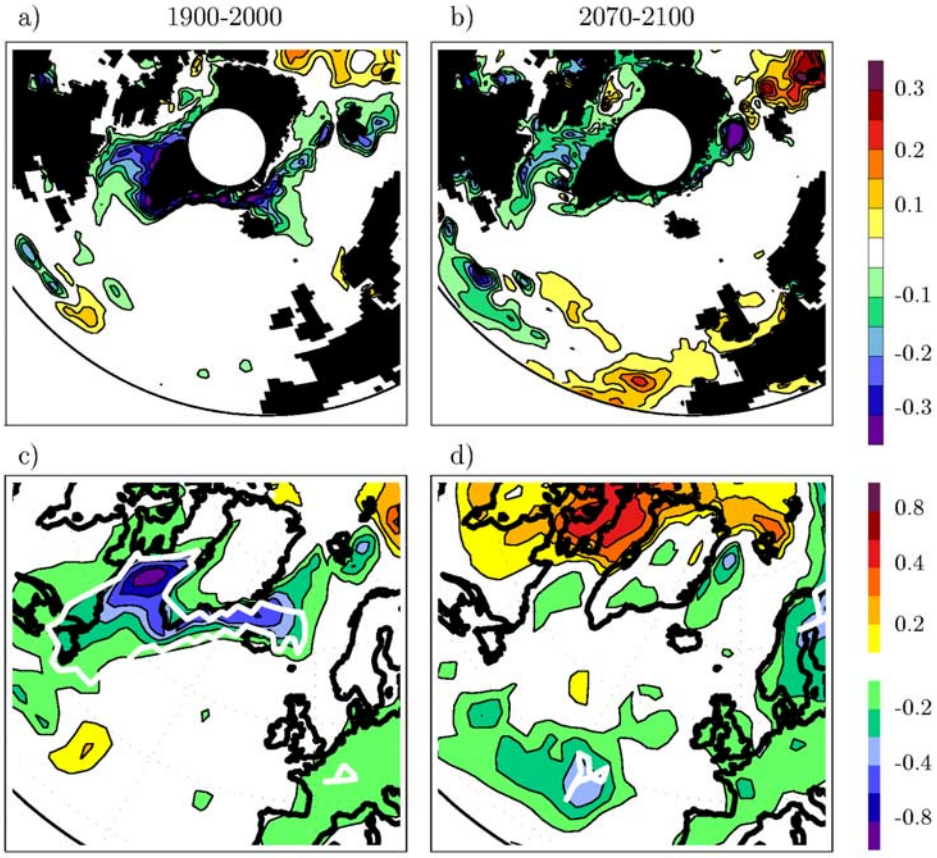

Figure 10. (a and b) Annual mean salinity anomalies in psu and (c and d) 2 m air temperature in Kelvin for the periods (left) 1900–2000 and (right) 2070–2100 1 a after large freshwater exports through Fram Strait (exceeding mean plus 1 standard deviation). The white line in Figures 10c and 10d indicates the 95% significance level.

convection in the Labrador Sea while convection in the Greenland Sea remains stable. Although in our simulations a complete collapse in the Labrador Sea does not occur and changes in the Greenland Sea do happen, the results show the same tendency: the Labrador Sea convection is more sensitive to anthropogenic forcing than convection in the Greenland Sea.

[34] The reason for the decrease in convection in our simulations differs in the two areas. In the Labrador Sea, increasing P-E and increasing freshwater exports through Fram Strait until 2030 and through the Canadian Archipelago thereafter reduce the density of the ocean surface and consequently the convection. In the upper layers of the Greenland Sea, there is no enhanced freshwater input. Here it is mainly the very strong temperature increase of the ocean surface that reduces convection. The temperature plays a role in the Labrador Sea as well, but the warming is much stronger in the Greenland Sea (not shown).

[35] The deep water formation in the northern North Atlantic is crucial for the entire thermohaline circulation. The maximal Atlantic meridional overturning circulation (MOC) has a negative trend throughout the entire 21st century. The mean of the three realizations shows a reduction by 6 Sv, leading to a total MOC of 16 Sv by 2100 (Figure 9b). However, in none of the three ensemble runs does the MOC break down. *Schmittner et al.* [2005] used 28 projections from 9 coupled climate models to analyze the MOC in the A1B scenario for the 21st century. To reduce the model uncertainties, a weighting procedure was applied considering the skill of each model in simulating hydrographic properties and observation-based circulation estimates. Their analysis predicted a gradual weakening of the MOC by 25% until 2100.

[36] Besides the large-scale oceanic response to changes in the freshwater fluxes, there are also effects at regional scales. In a recent paper, *Koenigk et al.* [2006] showed that the variability of the freshwater export through Fram Strait has a significant impact on the climate in the Labrador Sea. A large freshwater anomaly, exported through Fram Strait, is propagating in the East Greenland Current to the south and into the Labrador Sea in about 1 a. This produces—similar to the formation of Great Salinity Anomalies [*Dickson et al.*, 1988; *Belkin et al.*, 1998]—a large negative salinity anomaly in the Labrador Sea, which strongly reduces convection there. The ocean surface is colder than usual and the ice cover increases. Consequently, the ocean heat release to the atmosphere is strongly reduced and the air temperature is significantly colder. To determine if this process is changing during the 21st century, surface salinity and air temperature are analyzed after large freshwater exports through Fram Strait in the 20th and at the end of the 21st century (2070–2100, Figure 10). Export events of

all three ensemble runs are considered. In the 20th century, the process described above is well reproduced. At the end of the 21st century, still a quite large salinity anomaly occurs but there is no significant response of the temperature anymore. The explanation is simple. As shown above, convection in the Labrador Sea is strongly reduced in the 21st century (Figure 9a). An additional freshwater input cannot reduce the convection anymore because it is already weak. Thus the process leading to the atmospheric response does not exist anymore.

4. Summary and Conclusions

[37] An ensemble of 20th century and A1B scenario runs for the 21st century has been used to investigate the changing freshwater export out of the Arctic Ocean. The Arctic is the area with the largest simulated climate changes of the entire earth in the 21st century. The warming is twice the warming of the global mean. Consequently, Arctic sea ice is strongly reduced and the Arctic is ice free during summertime at the end of the 21st century.

[38] The freshwater input into the Arctic Ocean is strongly enhanced. Both P-E and the river runoff contribute to this increase. This leads to an increased freshwater content of the Arctic Ocean. The freshwater is stored between surface and 250 m depth and is mainly concentrated in the Beaufort Sea and the Central Arctic. The total freshwater export is only slightly growing. However, there are strong changes in the distribution of the freshwater export. Generally, the ice export is dramatically reduced and almost zero at the end of the 21st century, while the liquid freshwater export increases. The total freshwater export trough Fram Strait does not show large changes during the 21st century while the export through the Canadian Archipelago is strongly enhanced. The different behavior can be explained by the loss of sea ice in the Arctic. As sea ice cannot be mixed with deeper layers of the ocean and has a larger velocity than water, the loss of sea ice leads to a reduced freshwater export. This affects particularly the freshwater export through Fram Strait because the largest sea ice export out of the Arctic takes place there. Furthermore, it is one of the reasons why most of the additional freshwater input into the Arctic Ocean is stored and not directly exported. Although sea level rise in the Arctic Ocean is larger than in the North Atlantic in the 21st century, the increased pressure gradient is not leading to a dramatically enhanced outflow. Equilibrium runs with constant forcing from year 2100 onward (not shown) suggest that the freshwater content in the Arctic Ocean has reached its maximum by 2120. Thereafter, the freshwater export through Fram Strait increases significantly, as well. A correlation analysis between both Fram Strait freshwater export and SLP as well as Canadian Archipelago freshwater export and SLP showed a strong dependence of the freshwater exports on the atmospheric circulation in the 20th century. The loss of sea ice leads to a reduction of this connection for the export through Fram Strait at the end of the 21st century.

[39] The interannual variability of the freshwater export through Fram Strait is dominated by the ice export until year 2030 and by the salinity variability of the exported water thereafter. It slightly decreases in the second half of the 21st century because of the reduced ice export, which is very sensitive to variations in the wind field. In contrast, the variability of the Canadian Archipelago export is strongly enhanced. It is mainly governed by variations of the volume flux through the Archipelago. The enhanced variability of the Canadian Archipelago export leads to a slight increase in the variability of the total Arctic export. Obviously, the relative importance of the Fram Strait freshwater export for the total Arctic export becomes smaller while the importance of the Canadian Archipelago grows. However, it is still under discussion how large the effect of a growing export through the Canadian Archipelago is for convection and overturning. *Myers* [2005] used a regional model and found that only a small part of the freshwater flow through the Canadian Archipelago is uptaken into the Labrador Seawater.

[40] Similar to this result, only a part of the freshwater exported through the Canadian Archipelago flows directly into the Labrador Sea convection area in our model. Nevertheless, this amount, which grows with increased Canadian Archipelago export, and a growing P-E lead to a freshened Labrador Sea. This effect, the warming in the 21st century and an enhanced freshwater flux through Fram Strait between 2020 and 2050 strongly reduce the convection. The convection in the Greenland Sea is also reduced but mainly because of strong surface warming. There is no additional freshwater flux into the Greenland Sea in the upper ocean. The MOC has a negative trend throughout the 21st century. It is reduced by 6 Sv until year 2100.

[41] In the 20th century, large freshwater exports through Fram Strait reduce convection in the Labrador Sea 1 and 2 a later. Consequently, sea ice cover is increased and the air above is significantly colder. This process does not exist anymore at the end of the 21st century because convection in Labrador Sea is substantially reduced.

[42] This study also indicates that the three A1B scenario runs for the 21st century differ for certain parameters and periods quite strongly. Therefore the use of ensemble simulations is highly recommended. The comparison of two different runs or periods (e.g., future versus present climate) may otherwise lead to wrong conclusions.

[43] **Acknowledgments.** This work was supported by the Deutsche Forschungsgemeinschaft through the Sonderforschungsbereich 512. The computations have been performed of the Deutsches Klima Rechenzentrum (DKRZ).

References

Aargaard, K., and E. Carmack (1989), The role of sea ice and other fresh water in the Arctic circulation, *J. Geophys. Res.*, *94*, 14,485–14,498.

Alexander, M., U. Bhatt, J. Walsh, M. Timlin, J. Miller, and J. Scott (2004), The atmospheric response to realistic Arctic sea ice anomalies in an AGCM during winter, *J. Clim.*, *17*, 890–905.

Arnell, N. (2005), Implications of climate change for freshwater inflows to the Arctic Ocean, *J. Geophys. Res.*, *110*, D07105, doi:10.1029/2004JD005348.

Belkin, I., S. Levitus, J. Antonov, and S.-A. Malmberg (1998), "Great Salinity Anomalies" in the North Atlantic, *Prog. Oceanogr.*, *41*, 1–68.

Berezovskaya, S., D. Yang, and D. L. Kane (2004), Compatibility analysis of precipitation and runoff trends over the large Siberian watersheds, *Geophys. Res. Lett.*, *31*, L21502, doi:10.1029/2004GL021277.

Berezovskaya, S., D. Q. Yang, and L. Hinzmann (2005), Long-term annual water balance analysis of the Lena River, *Global Planet. Change*, *48*, 84–95.

Cavalieri, D. J. (2002), A link between Fram Strait sea ice export and atmospheric planetary wave phase, *Geophys. Res. Lett.*, *29*(12), 1614, doi:10.1029/2002GL014684.

Cavalieri, D., and S. Häkkinen (2001), Arctic climate and atmospheric planetary waves, *Geophys. Res. Lett.*, *28*, 791–794.

Déry, S. J., and E. F. Wood (2005), Decreasing river discharge in northern Canada, *Geophys. Res. Lett.*, *32*, L10401, doi:10.1029/2005GL022845.

Dickson, R., J. Meincke, S.-A. Malmberg, and A. Lee (1988), The "Great Salinity Anomaly" in the northern North Atlantic, 1968–1982, *Progr. Oceanogr.*, *20*, 103–151.

Dickson, R., S. Dye, M. Karcher, J. Meincke, B. Rudels, and I. Yashayaev (2007), Current estimates of freshwater flux through Arctic and sub-Arctic seas, *Prog. Oceanogr.*, in press.

Dyurgerov, M., and C. Carter (2004), Observational evidence of increases in freshwater inflow to the Arctic Ocean, *Arct. Antarct. Alp. Res.*, *36*, 117–122.

Goosse, H., F. Selten, R. Haarsma, and J. Opstegh (2002), A mechanism of decadal variability of sea-ice volume in the Northern Hemisphere, *Clim. Dyn.*, *19*, 61–83.

Groves, D. G., and J. A. Francis (2002), Variability of the Arctic atmospheric moisture budget from TOVS satellite data, *J. Geophys. Res.*, *107*(D24), 4785, doi:10.1029/2002JD002285.

Haak, H., J. Jungclaus, U. Mikolajewicz, and M. Latif (2003), Formation and propagation of great salinity anomalies, *Geophys. Res. Lett.*, *30*(9), 1473, doi:10.1029/2003GL017065.

Hagemann, S., and L. Duemenil (1998), A parameterisation of the lateral waterflow for the global scale, *Clim. Dyn.*, *14*, 17–31.

Hagemann, S., and L. Duemenil-Gates (2003), Improving a subgrid runoff parameterisation scheme for climate models by the use of high resolution data derived from satellite observations, *Clim. Dyn.*, *21*, 349–359.

Häkkinen, S. (1999), A simulation of thermohaline effects of a great salinity anomaly, *J. Clim.*, *6*, 1781–1795.

Hilmer, M., and T. Jung (2000), Evidence for a recent change in the link between the North Atlantic Oscillation and Arctic sea ice export, *Geophys. Res. Lett.*, *27*, 989–992.

Hilmer, M., and P. Lemke (2000), On the decrease of Arctic sea ice volume, *Geophys. Res. Lett.*, *27*, 3752–3754.

Hilmer, M., M. Harder, and P. Lemke (1998), Sea ice transport: A highly variable link between Arctic and North Atlantic, *Geophys. Res. Lett.*, *25*, 3359–3362.

Holfort, J., and J. Meincke (2005), Time series of freshwater-transport on the East Greenland Shelf at 74°N, *Meteorol. Z.*, *14*, 703–710.

Holland, M., and C. Bitz (2003), Polar amplification of climate change in coupled models, *Clim. Dyn.*, *21*, 221–232.

Johannessen, O., C. Myrmehl, A.-M. Olsen, and T. Hamre (2002), Ice cover data analysis–Arctic, *AICSEX Tech. Rep. 2*, Nansen Environ. and Remote Sens. Cent., Bergen, Norway.

Jung, T., and M. Hilmer (2001), The link between the North Atlantic Oscillation and Arctic sea ice export, *J. Clim.*, *14*, 3932–3943.

Jungclaus, J., H. Haak, M. Latif, and U. Mikolajewicz (2005), Arctic–North Atlantic interactions and multidecadal variability of the meridional overturning circulation, *J. Clim.*, *18*, 4016–4034.

Jungclaus, J., M. Botzet, H. Haak, N. Keenlyside, J.-J. Lou, M. Latif, J. Marotzke, U. Mikolajewicz, and E. Roeckner (2006), Ocean circulation and tropical variability in the coupled model ECHAM5/MPI-OM, *J. Clim.*, *19*, 3952–3972.

Koenigk, T., U. Mikolajewicz, H. Haak, and J. Jungclaus (2006), Variability of Fram Strait sea ice export: Causes, impacts and feedbacks in a coupled climate model, *Clim. Dyn.*, *26*, 17–34, doi:10.107/s00382-005-0060-1.

Kwok, R. (2000), Recent changes in Arctic Ocean sea ice motion associated with the North Atlantic Oscillation, *Geophys. Res. Lett.*, *27*, 775–778.

Lammers, R., A. Shiklomanov, C. Vorosmarty, B. Fekete, and B. Petersen (2001), Assessment of contemporary Arctic river runoff based on observational discharge records, *J. Geophys. Res.*, *106*, 3327–3334.

Magnusdottir, G., C. Deser, and R. Saravanan (2004), The effects of North Atlantic SST and sea ice anomalies on the winter circulation in CCM3. part 1: Main features and storm track characteristics of the response, *J. Clim.*, *17*, 857–876.

Manabe, S., P. Milly, and R. Weatherald (2004), Simulated long-term changes in river discharge and soil moisture due to global warming, *Hydrol. Sci. J.*, *49*, 625–642.

Marsland, S., H. Haak, J. Jungclaus, M. Latif, and F. Roeske (2003), The Max Planck Institute global ocean/sea ice model with orthogonal curvilinear coordinates, *Ocean Modell.*, *5*, 91–127.

Mauritzen, C., and S. Häkkinen (1997), Influence of sea ice on the thermohaline circulation in the Arctic–North Atlantic Ocean, *Geophys. Res. Lett.*, *24*, 3257–3260.

McClelland, J., R. M. Holmes, B. Peterson, and M. Stieglitz (2004), Increasing river discharge in the Eurasian Arctic: Consideration of dams, permafrost thaw and fires as potential agents of change, *J. Geophys. Res.*, *109*, D18102, doi:10.1029/2004JD004583.

McClelland, J., S. Dery, B. Peterson, and R. M. Holmes (2006), A pan-Arctic evaluation of changes in river discharge during the latter half of the 20th century, *Geophys. Res. Lett.*, *33*, L06715, doi:10.1029/2006GL025753.

Myers, P. (2005), Impact of freshwater from the Canadian Arctic archipelago on Labrador Sea water formation, *Geophys. Res. Lett.*, *32*, L06605, doi:10.1029/2004GL022082.

Peterson, B., R. Holmes, J. McClelland, C. Vorosmarty, R. Lammers, A. Shiklmanov, I. Shiklomanov, and S. Rahmstorf (2002), Increasing river discharge to the Arctic Ocean, *Science*, *298*, 2171–2173.

Prinsenberg, S., and J. Hamilton (2005), Monitoring the volume, freshwater and heat fluxes passing through Lancaster Sound in the Canadian Arctic archipelago, *Atmos. Ocean*, *43*, 1–22.

Przybylak, R. (2002), Variability of total and solid precipitation, *Int. J. Climatol.*, *22*, 904–916.

Roeckner, E., et al. (2003), The atmosphere general circulation model ECHAM5, part 1: Model description, *Max Planck Inst. Meteorol. Rep. 349*, 127 pp., Max Planck Inst., Munich, Germany.

Schmith, T., and C. Hansen (2003), Fram Strait ice export during 19th and 20th centuries: Evidence for multidecadal variability, *J. Clim.*, *16*, 2782–2791.

Schmittner, A., M. Latif, and B. Schneider (2005), Model projections of the North Atlantic thermohaline circulation for the 21st century assessed by observations, *Geophys. Res. Lett.*, *32*, L23710, doi:10.1029/2005GL024368.

Serreze, M., R. Barry, and J. Walsh (1995), Atmospheric water vapor characteristics at 70°N, *J. Clim.*, *8*, 719–731.

Serreze, M., J. Walsh, F. S. Chapin III, T. Osterkamp, V. Romanovsky, W. Oechel, J. Morison, T. Zhang, and R. Barry (2000), Observational evidence for recent climate change in the northern high-latitude environment, *Clim. Change*, *46*, 159–207.

Valcke, S., A. Caubel, D. Declat, and L. Terray (2003), OASIS Ocean Atmosphere Sea Ice Soil user's guide, *Tech. Rep. TR/GMGC/03/69*, 85 pp., Cent. Eur. Formation Avancee Calcul Sci., Toulouse, France.

Vinje, T. (2001), Fram Strait ice effluxes and atmospheric circulation 1950–2000, *J. Clim.*, *14*, 3508–3517.

Vinje, T., N. Nordlund, and A. Kvambeck (1998), Monitoring ice thickness in Fram Strait, *J. Geophys. Res.*, *103*, 10,437–10,449.

Walsh, J., X. Zhou, D. Portis, and V. Meleshko (1994), Atmospheric contribution to hydrologic variations in the Arctic, *Atmos. Ocean*, *34*, 733–755.

Wood, R., A. Keen, J. Mitchell, and J. Gregory (1999), Changing spatial structure of the thermohaline circulation in response to atmospheric CO_2 forcing in a climate model, *Nature*, *399*, 572–575.

Woodgate, R., and K. Aagaard (2005), Revising the Bering Strait freshwater flux into the Arctic Ocean, *Geophys. Res. Lett.*, *32*, L02602, doi:10.1029/2004GL021747.

Wu, P., R. Wood, and P. Scott (2005), Human influence on increasing Arctic river discharges, *Geophys. Res. Lett.*, *32*, L02703, doi:10.1029/2004GL021570.

H. Haak, J. Jungclaus, T. Koenigk, and U. Mikolajewicz, Max-Planck-Institut für Meteorologie, Bundesstraße 53, D-20146 Hamburg, Germany. (torben.koenigk@zmaw.de)